2011 International Conference on Computer Science and Information Technology (ICCSIT 2011)
IPCSIT vol. 51 (2012) © (2012) IACSIT Press, Singapore
DOI: 10.7763/IPCSIT.2012.V51.20

Image Segmentation of Cerebrospinal Fluid Using a New Hybrid Level-Set Model

Jinghua Zhu[a], Ying Ju[a,*]

[a] Computer Science Department, Xiamen University, Xiamen 361005, China

Abstract. It is very significant for medical diagnosis to get the correct boundary of cerebrospinal fluid (CSF) space in brain Magnetic Resonance (MR) images. In this paper, a new hybrid active contour model in the level-set framework for medical image segmentation was presented. The model is the hybrid of boundary-based and region-based. The boundaries of target objects can be extracted with the model straightforwardly requiring no preprocessing. The experimental results show that the proposed method is efficient.

Keywords: CSF,MRI,active contour model, level-set, image segmentation

1. Introduction

Cerebrospinal fluid (CSF) is a clear liquid produced mainly in the choroid plexus of brain. The normal flow of CSF is very important to maintain the intracranial pressure to the normal level. If obstruction or blockage occurs in the flow of CSF, it may cause some illness such as Hydrocephalus. In recent years, the researches on the computational simulation of CSF system are helpful to diagnose the CSF disorder and to make treatment planning [1], [2], [3].Yet the correctness of the results in these computational simulations relies on the accuracy of geometric boundary of CSF. Therefore, the accurate estimation of CSF boundary has its clinical meanings such as the treatment planning or therapy evaluation for Hydrocephalus. One of efficient methods to estimate CSF boundary is segmentation of CSF based on brain image.

Since active contour models were originally proposed in [4], the researches on active contour models for brain image segmentation have been popular in recent years [5], [6], [7]. Active contour models are based on the theory of curve evolution, namely evolving the initial curve towards the boundaries of target objects via minimizing the functional which should be designed that the curves close to boundaries have low values. The contours can be represented either explicitly or implicitly. Their typical representations are parametric model and level-set model respectively. Between these two categories of models, the level-set model becomes the state of the art due to its many distinguished advantages as following: 1) It can handle complicate geometries and change topology automatically.2) the algorithm is able to be extended to 3D easily.3) its numerical implementation is very easy.

In the framework of level-set, the active contour models can be classified into three categories: boundary-based [8], region-based [9], and hybrid of boundary-based and region-based [10]. The boundary-based model is sensitive to the definition of the target boundary, and the region-based model can not be guaranteed to detect the target boundary accurately. Zhang model in [10] has overcome these two shortcomings to be an excellent method of medical image segmentation. However, Zhang model is just expert in segmenting the object which has highest gray-level or lowest gray-level, but for other situations, it may have some problems. One of the key contributions of this paper is overcoming this difficult. Without any preprocessing of original

* Corresponding author. *E-mail address*: yju@xmu.edu.cn.

images, the proposed method is applied straightforwardly for the purpose of CSF segmentation and gets the proper results.

2. Method

2.1. Level-set method

In the level-set framework, the active contour is defined in an implicit form as follows:

$$C(t) = \{(x, y) \in \Omega \mid \phi(x, y, t) = 0\} \tag{1}$$

where Ω is image domain and ϕ is the level-set function, which should agree with:

$$\begin{cases} \phi(x, y) = 0, & (x, y) \in C \\ \phi(x, y) > 0, & (x, y)\ inside\ C \\ \phi(x, y) < 0, & (x, y)\ \ outside\ C \end{cases} \tag{2}$$

Here ϕ is defined to be signed distance function (SDF),

$$|\phi(p)| = \min(d(p, p_i)), \quad p_i \in C \tag{3}$$

where d is Euclidean distance. There is an significant feature for such level-set function, i.e. $|\phi|=1$.

The curve or surface evolution is driven by minimizing the functional whose value is lowest as the curve or surface meets the boundary to be detected. Take the geodesic contour model for example. Its functional is defined as follows:

$$\varepsilon(\phi) = \int_{\Omega} g \mid \nabla H(\phi) \mid d\Omega \tag{4}$$

where g is a decreasing function of image gradient, and H is Heaviside function.

$$H(\phi) = \begin{cases} 0, \ if\ \phi < 0 \\ 1, \ if\ \phi \geq 0 \end{cases}, \tag{5}$$

It's clear that minimizing the functional (4) is able to push the contour towards the positions with high image gradients. To minimize the functional, Gateaux derivative gradient flow is applied to (4), which gives rise to the following partial differential equation (PDE),

$$\phi_t = \mid \nabla\phi \mid div(g \nabla\phi / \mid \nabla\phi \mid) \tag{6}$$

This PDE is the curve evolution function. Solving it will result in the final contour which attaches to the boundary of target object.

In general, the curve evolution function can be written as,

$$dC/dt = C_t = F\vec{N} \tag{7}$$

Where F is speed function, $\vec{N}$ is the unit normal of the curve. In level-set model, $\vec{N} = \nabla\phi/|\nabla\phi|$. It can be proved easily that the curve evolution PDE is formulated as,

$$\phi_t = \mid \nabla\phi \mid F \tag{8}$$

The process of the proving is as follows,

$$\phi_t = \langle C_t, \nabla\phi \rangle = \left\langle F\vec{N}, \nabla\phi \right\rangle = \left\langle \frac{\nabla\phi}{|\nabla\phi|}, \nabla\phi \right\rangle F = \mid \nabla\phi \mid F$$

where " < , >" represents inner product.

2.2. The new hybrid method of boundary-based and region-based

The functional of the hybrid method is the combinations of region information and boundary information. The functional of the proposed new hybrid method is designed as:

$$\varepsilon(\phi) = -\alpha\int_{\Omega} f(I)H(\phi)d\Omega + \beta\int_{\Omega} g \mid \nabla H(\phi) \mid d\Omega \tag{9}$$

where Ω is the image domain, both α and β are positive constant which are designed to balance these two terms. *H* is the Heaviside function defined in (5).And *g* is a decreasing function of image gradient, here it is defined as $g = \exp(-c|\nabla I|^2)$. Moreover, the region information function *f (I)* is defined as,

$$f(I) = -(I - (\mu_1 + \mu_2)/2)^2 + (\mu_1 - \mu_2/2)^2 \quad (10)$$

where *I* is the image to be segmented, $\mu 1$ and $\mu 2$ represent lower bound gray-level and upper bound gray-level of the target object respectively.

As shown in Fig. 1, the value of function *f* is above zero if the value of *I* is between $\mu 1$ and $\mu 2$. Otherwise, *f* is below zero. This feature of the function *f* ensures that minimizing the first term of functional (9) amounts to encouraging the contours to enclose the regions whose gray-level is between $\mu 1$ and $\mu 2$. The second term is employed to drive the contour to move towards higher image gradient.

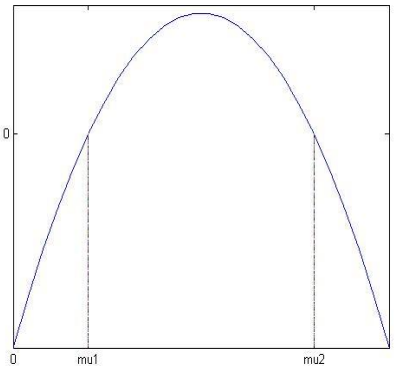

Fig. 1. The graph of region information function *f(I)*

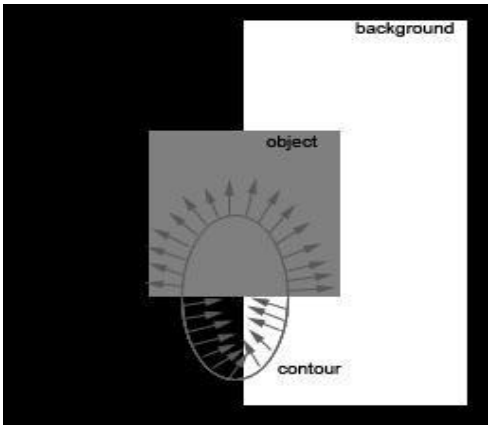

Fig. 2. Contour deforming in normal direction

Minimizing the functional (9), the associated PDE is deduced,

$$\phi_t = |\nabla\phi|(\alpha f(I) + \beta div(g \nabla\phi/|\nabla\phi|)) \quad (11)$$

According to the formulation (8), the speed function is derived,

$$F = \alpha f(I) + \beta div(g \nabla\phi/|\nabla\phi|) \quad (12)$$

The contours deform in the normal directions with the speed of *F*. The first term of *F* is positive for the parts of the contour inside the target object, and negative for the parts outside the target object. It's well known that the positive normal direction is defined to point outward. So it means that the parts of contour inside target object spread, and the outside parts shrink (see Fig. 2). The role of the second term is to encourage the contours to move towards the higher image gradient.

Since the level-set function is defined as SDF. The PDE (11) can be simplified as,

$$\phi_t = \alpha f(I) + \beta div(g \nabla\phi/|\nabla\phi|) \quad (13)$$

A stable iterative numerical scheme for solving the PDE can be seen in [10].

3. Experimental results

To prove the efficiency of the proposed model, the model has been tested on both synthetic image and real brain MR images. Firstly, the synthetic image shown in Fig.3 (a) is contaminated by Gaussian noise. The triangle is the target object to be segmented, whose gray-level is lower than the rectangle but higher

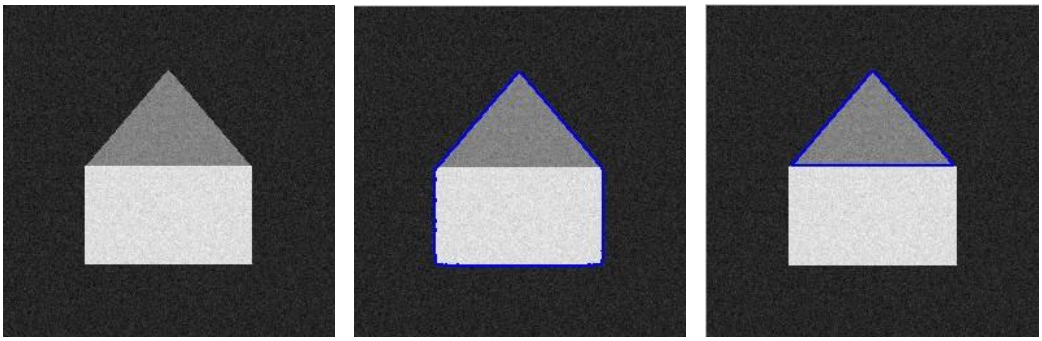

(a) Synthetic image (b) Result of Zhang model (c) Result of the proposed model

Fig.3. Comparison with Zhang model on synthetic image

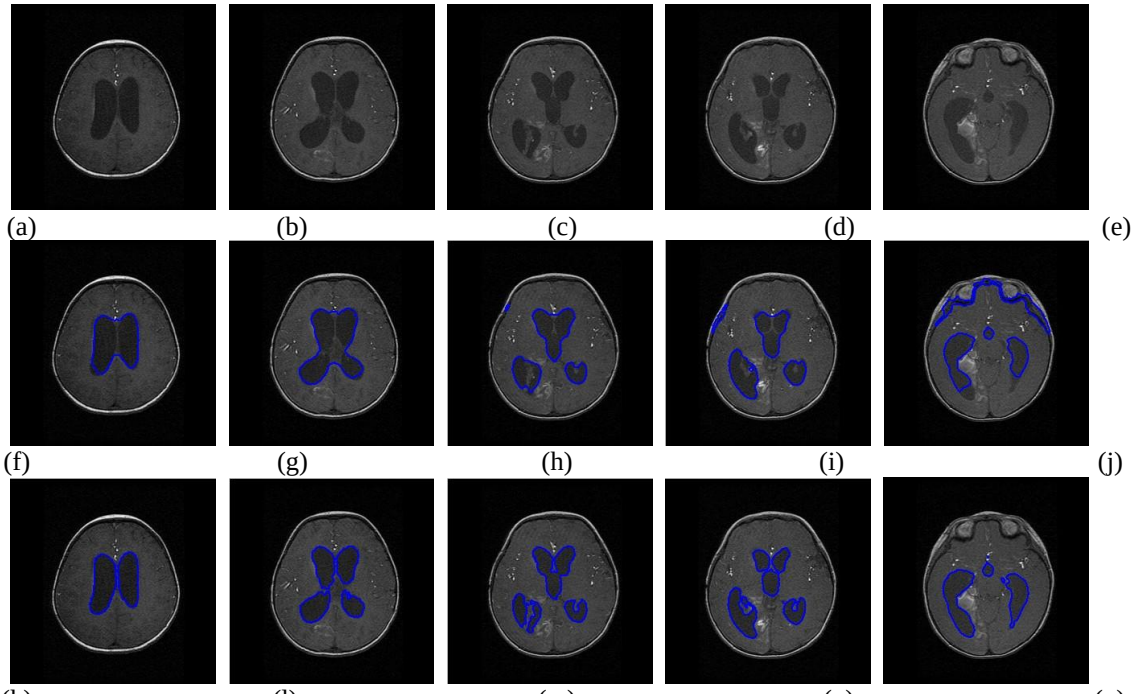

(a) (b) (c) (d) (e)

(f) (g) (h) (i) (j)

(k) (l) (m) (n) (o)

Fig.4. Comparisons with Zhang model in Segmenting CSF based on brain MR images

than the background. As shown in Fig.3 (b), Zhang model fails to detect the accurate boundary of the triangle. The reason is very simple. In Zhang model, only the objects with higher or lower gray-level can be detected. Thus, enclosing the triangle which has middle gray-level, the contour encloses unavoidably the rectangle. Fig.3 (c) shows that the proposed model can segment the triangle correctly.

Besides, the new hybrid model was also tested on 66 slices of real brain MR images of size 256×256 supplied by Beijing general navy hospital. Five typical slices of these brain images shown in Fig.4 (a) ~ (e) are chosen to present the efficiency of the proposed model. The segmentation results of Zhang model are shown in Fig.4 (f) ~ (j), and the final results of the proposed model are shown in Fig.4 (k) ~ (o). As presented in Fig.4 (f) ~ (j), the Zhang model can not extract the CSF in ventricles accurately. The final contours computed by Zhang model fail to partition the isolated regions. What's more, Fig.4 (h) ~ (j) show that Zhang model segmented some extra brain tissues. Fig.4 (k) ~ (o) illustrate that the proposed model do well in detecting the boundaries of CSF in ventricles. The contours attach to the exact boundaries of CSF without enclosing other extra tissues, and separate all of the isolated parts.

In fact, the final results are converged to by the proposed model faster than Zhang model. In the experiment of synthetic image segmentation, only 5 iterations were consumed by the proposed model to converge to the right result, but 13 iterations were needed by Zhang model to converge to the wrong result. In addition, the similar thing occurred in the CSF segmentation experiment. In the best case, the result shown in Fig.4 (k) was produced just in 7 iterations by the proposed model. And in the worst case, 12 iterations were required to get the result in Fig.4 (n). However, 10 iterations were consumed in the result shown in Fig.4 (g)

which is converged to fastest by Zhang model. What's worse, 92 iterations were consumed in the result shown in Fig.4 (j) by Zhang model.

4. Conclusion

It has been proved in Section 3 that the proposed method is efficient in extracting the boundaries of the object whose rough gray-level range is known. Actually, it can be extensively applied in medical image segmentation. Furthermore, no preprocessing is required in the process of segmenting with the proposed method. The only drawback of the proposed method is that the approximate gray-level range of target object needs to be estimated in advance. The focus of the next step will be on overcoming it.

5. Acknowledgements

The work in this paper has been supported by the National Nature Science Foundation of China (61071151).

6. References

[1] A. Smillie, I. Sobey, and Z. Molnar, "A hydroelastic model of hydrocephalus, " Journal of Fluid Mechanics, 539: pp. 417-443, 2005.

[2] X. Shen, G. Narsilio, H. Wang, D. Smith, G. Egan, "Using numerical model to predict hydrocephalus based on MRI images, " in Proc. Jt. Meet. Int. Symp. Noninvasive Funct. Source Imaging Brain Heart Int. Conf. Funct. Biomed. Imaging, NFSI and ICFBI, pp.51-54, 2007.

[3] V. Kurtcuoglu, M. Soellinger, P. Summers, K. Boomsma, D. Poulikakos, et al., "Reconstruction of cerebrospinal fluid flow in the third ventricle based on MRI data, " In 8th International Conference on Medical Image Computing and Computer-Assisted Intervention, pp.786-793,2005.

[4] M. Kass, A. Witkin and D. Terzopoulos. "Snakes: Active contour models, " International Journal of Computer Vision, 1:321-331, 1988.

[5] A. Huang, R. Abugharbieh , R. Tam, A. Traboulsee, "MRI Brain Extraction with Combined Expectation Maximization and Geodesic Active Contours, " In: SP&IT, IEEE International Symposium, August 2006, pp. 107 - 111 (2006).

[6] W. Cho, J. Park, S. Park, S. Kim, S. Kim, et al., "Level-Set Segmentation of Brain Tumors using a New Hybrid Speed Function," In Proc. Int. Conf. Pattern Recognit., pp.1545-1548, 2010.

[7] M. Hacini, F. Hachouf, "MR Image Segmentation Based on a New Hybrid Level Set Evolution, "In Int. Conf. Inf. Sci., Signal Process. Appl., ISSPA, pp.444-447,2010.

[8] R. Goldenberg, R. Kimmel, E. Rivlin and M. Rudzsky. "Fast geodesic active contours," IEEE Transactions on Image Processing, 10(10):1467-1475, 2001.

[9] T. F. Chan, L. A. Vese, "Active contours without edges, " IEEE Transactions on Image Processing, 10(2):266-277, 2001.

[10] Y. Zhang, B. J. Matuszewski, L.-K. Shark, C.J. Moore, "Medical Image Segmentation Using New Hybrid Level-Set Method, " In proceedings of MediViz Conference, IEEE, pp.71-76, 2008.